Electrical circuit models for performance modeling of Lithium-Sulfur batteries

Knap, Vaclav; Stroe, Daniel-Ioan; Teodorescu, Remus; Swierczynski, Maciej Jozef; Stanciu, Tiberiu

Published in:
Proceedings of the 2015 IEEE Energy Conversion Congress and Exposition (ECCE)

DOI (link to publication from Publisher):
10.1109/ECCE.2015.7309853

Publication date:
2015

Document Version
Early version, also known as pre-print

Electrical Circuit Models for Performance Modeling of Lithium-Sulfur Batteries

Vaclav Knap, Daniel-Ioan Stroe, Remus Teodorescu, Maciej Swierczynski and Tiberiu Stanciu
Department of Energy Technology, Aalborg University
Aalborg, Denmark
Email: vkn@et.aau.dk

***Abstract*—Energy storage technologies such as Lithium-ion (Li-ion) batteries are widely used in the present effort to move towards more ecological solutions in sectors like transportation or renewable-energy integration. However, today's Li-ion batteries are reaching their limits and not all demands of the industry are met yet. Therefore, researchers focus on alternative battery chemistries as Lithium-Sulfur (Li-S), which have a huge potential due to their high theoretical specific capacity (approx. 1675 Ah/kg) and theoretical energy density of almost 2600 Wh/kg. To analyze the suitability of this new emerging technology for various applications, there is a need for Li-S battery performance model; however, developing such models represents a challenging task due to batteries' complex ongoing chemical reactions. Therefore, the literature review was performed to summarize electrical circuit models (ECMs) used for modeling the performance behavior of Li-S batteries. The studied Li-S pouch cell was tested in the laboratory in order to parametrize four basic ECM topologies. These topologies were compared by analyzing their voltage estimation accuracy values, which were obtained for different battery current profiles. Based on these results, the 3 R-C ECM was chosen and the Li-S battery cell discharging performance model with current dependent parameters was derived and validated.**

Keywords*—Electrical circuit model, Lithium-Sulfur battery, performance modeling, validation.

I. Introduction

Because of the ongoing demand for better batteries and since today's Lithium-ion (Li-ion) batteries are close to their limits, many researches focus on new battery chemistries and compositions. Lithium-Sulfur (Li-S) batteries get a high interest as they have a high theoretical specific capacity and theoretical energy density. This, introduced to the practice, will result in lighter batteries with higher capacity. Moreover, in comparison with Li-ion batteries, the production cost and environmental impact of the Li-S batteries would be positively influenced due to the usage of sulfur instead of other (rare) metals [1].

Li-S batteries are currently entering the market, yet with their parameters far from their theoretical limits. For their suitability selection to specific applications, it is necessary to evaluate their performance under various operation conditions (e.g. temperature, state-of-charge (SOC) or current). Moreover, the development of appropriate battery management system is required. Therefore, deriving of the performance model for the Li-S battery seems as an inevitable step. This activity should be done with consideration that the model should have relatively low computational effort as it might run online in specific applications. For such purposes, it is commonly used an equivalent circuit model (ECM), which is composed of fundamental electrical components (e.g. voltage sources, resistors, capacitors etc.) and it is straightforward to integrate with other electrical system models (e.g. an electric vehicle or an energy storage in a grid) [2]–[4].

In order to achieve high accuracy of the performance model, a suitable ECM topology has to be selected. This topology might be different from the ones used for Li-ion batteries, as the Li-S battery has more complex chemical reactions [5]. So far, there were only few activities reported in literature regarding the development of ECM for performance modeling of Li-S batteries [6], [7], which used 2 R-C ECM topology. Most of the Li-S ECMs in literature are used for electrochemical analysis by electrochemical impedance spectroscopy [8]–[14] and they do not directly results to the performance model.

This paper presents a summary of various ECM topologies for Li-S batteries, together with the considered parameter dependencies and the used parametrization methods. Based on this review, four basic ECM topologies with 1 R-C to 4 R-C elements were chosen and parametrized based on laboratory measurements performed on a 3.4 Ah Li-S pouch cell. The topologies are compared according to their accuracy in fitting and their voltage estimation error.. Furthermore, one ECM topology is selected and the Li-S battery cell discharging performance model with current dependent parameters is developed and validated.

The paper is structured as follows: Li-S battery fundamentals are introduced in Section II. Section III presents the summary of ECMs for Li-S batteries. The methodology, including modeling, parametrization, comparison and validation, is described in Section IV. Section V presents and discusses the main obtained results. The conclusions are drawn in Section VI.

II. Lithium-Sulfur Battery

Typically, a Li-S battery consists of a lithium anode, a sulfur composite cathode, a polymer or liquid electrolyte and a separator. Moreover, additives and binders are used to improve the battery characteristics. Based on the electrodes' properties, a Li-S battery has a high theoretical specific capacity of around 1675 Ah/kg and a theoretical energy density close to 2600 Wh/kg. These characteristics outnumber conventional Li-ion batteries with their theoretical specific capacity of 155 Ah/kg and theoretical specific energy of up to 570 Wh/kg [1], [15].

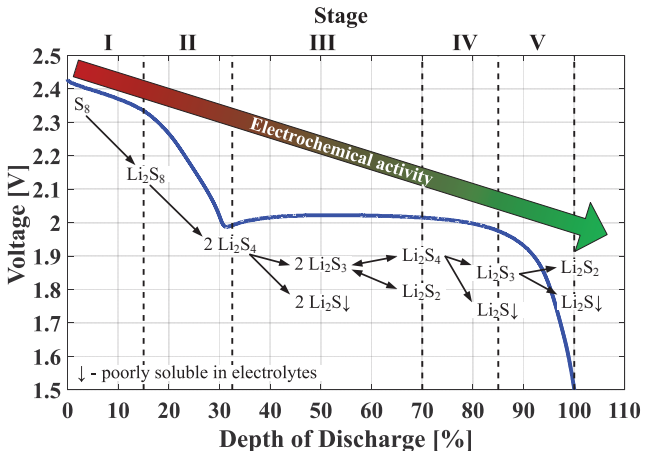

Fig. 1. Typical Li-S discharge voltage curve with illustrated stages and poly-sulfide reactions.

Li-S batteries are characterized by more complicated internal chemical reactions than today's Li-ion batteries. During usage, sulfur goes through different stages of poly-sulfides (Li_2S_n), which influences the battery electrochemical activity. The typical discharging voltage profile of a Li-S battery cell is shown in Fig. 1, together with illustrated stages and their associated prevailing reactions [5]. During discharging, lithium metal reacts with sulfur (S_8) and they form long chain poly-sulfides, which are further decomposed to short chain poly-sulfides. The final discharging product is Li_2S, which has the lowest electrochemical activity and it is insoluble in electrolytes. When Li_2S is produced, it deposits on the carbon, reducing carbon accessibility, and by that the cathode active surface area is reduced [5], [15]. Charging is the opposite process to discharging and poly-sulfide chains are formed from shorter to longer ones. However, the long chain poly-sulfides are highly soluble in electrolytes and during the high charged stages they diffuse to the lithium anode, where they react with the lithium and they are reduced to short chain poly-sulfides, which diffuse back to the cathode. This phenomenon is called "poly-sulfide shuttle" and it causes internal resistance growth, fast capacity decrease, low coulombic efficiency, and high self-discharge. However, the poly-sulfide shuttle provides also a beneficial attribute of an inherent overcharge protection [1], [16].

III. Equivalent Circuit Models for Lithium-Sulfur Batteries

The structure of ECMs can differ depending on the modeled battery chemistry, targeted application and desired accuracy. A general ECM is shown in Fig. 2. It consists of a voltage source representing the open-circuit voltage (OCV) and impedance elements. The simplest ECM topology is a resistance model, which contains only one resistor in series. The clear benefit of this approach is its minimal computation requirements and simplicity, however it provides the lowest accuracy [3], [4].

In literature, the proposed ECMs for Li-S batteries are composed of resistors, capacitors, constant phase angle elements (CPEs) and Warburg impedance. Typically, CPEs are used to take into account a non-ideal behaviour of an electrode, like

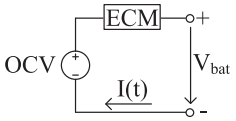

Fig. 2. A general equivalent electrical circuit.

a roughness of the surface and porosity of a material [8]. Using CPEs and Wargburg impedance elements give better fitting accuracy. Nevertheless, they are often later on approximated with parallel R-C elements to reduce the computation effort. Thus, this paper focuses the investigation on evaluating parallel R-C elements-based ECMs, where CPEs are replaced by capacitors. The main ECM structures used to model the dynamic behaviour of Li-S batteries are shown in Fig. 3; a voltage source representing OCV is not shown, but is assumed to be part of every discussed ECM. Moreover in literature, these topologies are sometimes expanded by and additional Warburg impedance or a capacitor. These ECMs are considered as subtypes of the main structures and they are not further considered in this paper.

Overall, the ECMs for a Li-S battery are composed of a series resistance and from one to four R-C parallel elements. The elements of the circuits usually represent some specific physical attributes and processes in the battery. In ECM 1, R0, R1 and C1 stands for the resistance of the electrolyte, the charge transfer resistance and the double-layer capacitance, respectively [9]. ECM 2 expands ECM 1 with R2 and C2, which express total resistance and distributed capacitance of the surface layers of both the sulfur and lithium electrodes according [13]. However, in literature, the related meaning of some ECM components varies according to used identification methods, assumptions of authors, and specific cell composition; for example in [10], R2 is connected to the nafion film resistance, as the nafion membrane coating is additionally used on the electrode surface. In a similar way related to ECM 4, authors in [17] redefine and adjust the meaning of elements that R0 is associated to the ohmic resistance caused by the

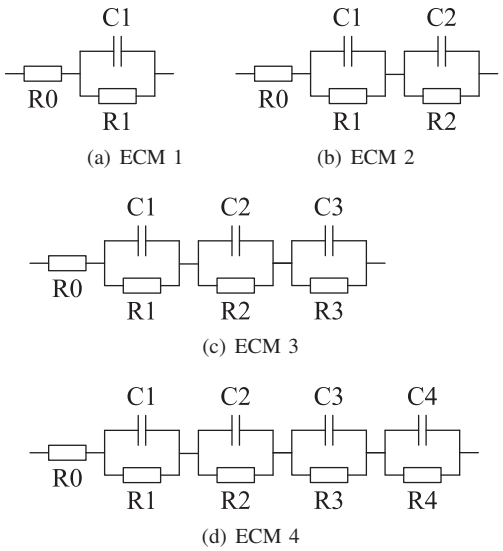

(a) ECM 1 (b) ECM 2

(c) ECM 3

(d) ECM 4

Fig. 3. Main layouts of the ECMs for Li-S batteries.

TABLE I. SUMMARY OF ECMS FOR LI-S BATTERIES.

ECM Type	Parametriz--ation	Performance model	Reference
ECM 1	EIS	-	[8]–[12]
ECM 2	EIS, Pulse [6]	Yes [6], [7]	[6], [7], [9], [10], [13], [14]
ECM 3	EIS	-	[18]
ECM 4	EIS	-	[17]

TABLE II. DEPENDENCIES OF LI-S ECM PARAMETERS

Model type → / Dependencies ↓	ECM 1	ECM 2	ECM 3	ECM 4
SOC	[8], [9], [11]	[6], [7], [13]	-	[17]
Temperature	-	[6], [7]	-	-
C-rate	-	[6]	-	-
Cycle	[11], [12]	[7]	[18]	[17]
Calendar	[12]	[14]	-	-

electrolyte resistance, current collectors and cell connections. Moreover, R1-C1 is limited here to express only the charge transfer at the anode surface and the charge transfer of sulfur intermediates is represent by R2-C2. R3-C3 is related to the formation and dissolution of S_8 and Li_2S. In low frequency region, there appear diffusion processes, which are assigned to R4-C4.

Table I summarizes the ECMs, together with their references and parametrization methods. In majority of the cases, an ECM was used for investigation of electrochemical properties of a Li-S cell, if such model was created as a performance/impedance model; it is also mentioned in Table I. As it is shown, only ECM 2 was proposed to function as a performance model and it was also validated [6].

In Table II, there are summarized the dependencies of ECM parameters, which were examined by various researches for the main structures of the ECMs. ECM 2 is the most often investigated circuit, as it includes all parameter dependencies: on state-of-charge (SOC), temperature, C-rate, and age (cycle and calendar).

Based on the literature review, ECM 2 layout appears as the most often used topology for modeling of a Li-S cell. It is followed by ECM 1, which is simplified by removing one R-C element. This reduction can decrease the computation complexity, but as a drawback the obtained model accuracy will be lower. On the other hand, by adding one or two parallel R-C elements, ECM 3 and ECM 4 configurations are obtained, which offer better accuracy at the cost of higher computation demand.

IV. METHODOLOGY

The 3.4 Ah Li-S pouch cell, supplied by OXIS Energy, was placed in a temperature chamber, where it was connected to the Digatron battery test station as shown in Fig. 4. The temperature in the chamber was maintained at 35°C.

A series of tests were applied to the battery cell in order to parametrize the ECM model and to validate it. The discharging cut-off voltage is considered as 1.5 V (SOC=0%) and charging cut-off voltage is 2.45 V (SOC=100%). A general procedure consists of a preconditioning cycle (0.1 C-rate charging (CHA), 0.2 C-rate discharging (DCH)), a capacity check (0.1 C-rate

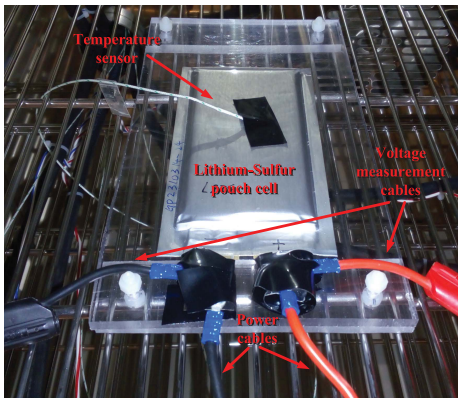

Fig. 4. Illustration of the Li-S battery cell during laboratory measurements.

CHA, x C-rate DCH, where x=0.2, 0.35, 0.5, 0.75 and 1.0 C-rate), another nominal cycle and full charging before applying a galvanostatic intermittent titration technique (GITT) [19]. The depth-of-discharge (DOD) steps for the GITT were computed from the measured capacity with a resolution of 2.5% and 5% resolution. The relaxation time between the steps was set to 30 minutes long; exceptions were considered for 0, 5, 10, and 15% DOD where the relaxation times were set to 1.5, 8, 15, and 21 minutes, respectively. This procedure was considered in order to decrease the influence of self-discharge in these low DOD regions.

A. Modeling

The model of the Li-S battery cell was implemented in Simulink according to the procedure discussed in [20]. The OCV and the circuit parameters are implemented as look-up tables, which considers their dependance on C-rate and DOD. For the C-rate dependance, the memory block is applied, which in the case of I=0 A keeps the last used value of C-rate as an input to the look-up tables. The model is considered only for the discharging case and it starts from the fully charged state (100% SOC). The SOC and DOD are calculated as follows:

$$SOC = SOC_{ini} + \int \frac{I \cdot 100}{C_{meas} \cdot 3600} dt, \tag{1}$$

$$DOD = 100 - SOC, \tag{2}$$

where SOC is battery state-of-charge in percentage, SOC_{ini} is the initial state-of-charge value, I is the current in Amperes, C_{meas} stands for measured capacity during the capacity check in amper-hours and DOD represents depth-of-discharge in percentage.

B. ECM parametrization and topology comparison

The ECM topology comparison is based on fitting 0.2, 0.5 and 1.0 C-rate GITT measurements separately to the 1-4 R-C ECM topologies. The voltage and current profiles for 0.2 C-rate are presented in Fig. 5. The OCV is derived from the relaxation period: a) from the maximum voltage for low DOD states, where the influence of self-discharge is very pronounced (illustrated in Fig. 5); b) from the voltage after 30 minutes relaxation period for higher DODs where voltage is increasing

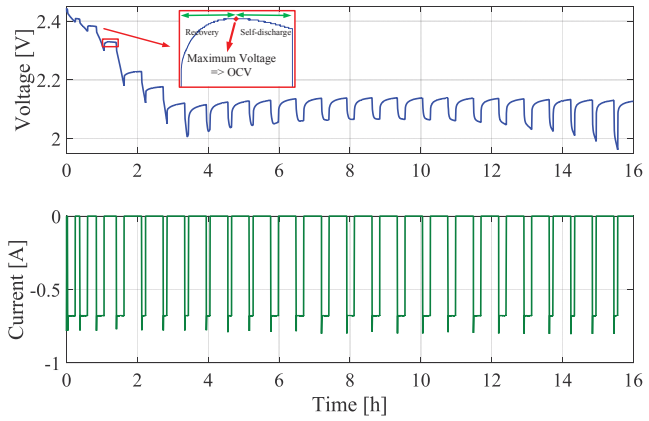

Fig. 5. GITT procedure for discharging of the Li-S cell by 0.2 C-rate [21].

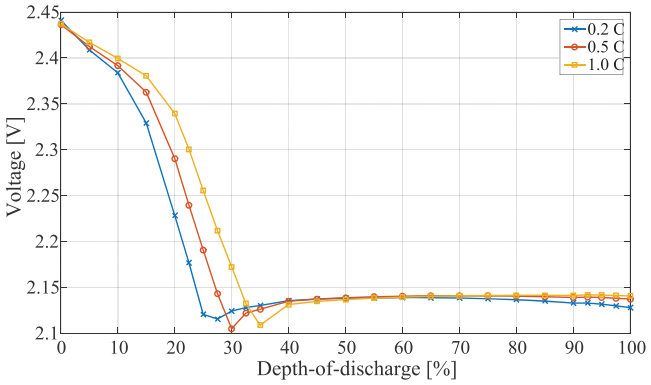

Fig. 6. Open-circuit voltage of the Li-S cell derived from the relaxation voltage of GITT for discharging steps.

during the recovery stage [21]. The obtained OCV curves in function of DOD are shown in Fig. 6.

The ECMs were parametrized following the PT3 technique, presented in [21], since it can be easily and quickly adapted to different number of R-C elements. R0 was determined from the instantaneous voltage drop, which follows after the current interruption as shown in Fig. 7. A least squares method was used to fit the measured relaxation voltage after the instantaneous voltage drop to:

$$V_{fit}(t) = OCV(DOD) - \sum_{i=1}^{n} U_i exp^{-t/\tau_i}, \tag{3}$$

where V_{fit} is the fitted voltage as a function of time t) OCV is the open-circuit voltage in function of DOD, U_i is the polarization voltage and τ_i is the time constant of i-th R-C element. The specific parameters R_i and C_i are extracted through:

$$R_i = \frac{U_i}{I_{cp}(1 - e^{-\frac{t_{cp}}{\tau_i}})}, \tag{4}$$

$$C_i = \frac{\tau_i}{R_i}, \tag{5}$$

where the current pulse amplitude is I_{cp} and duration of the current pulse is t_{cp}.

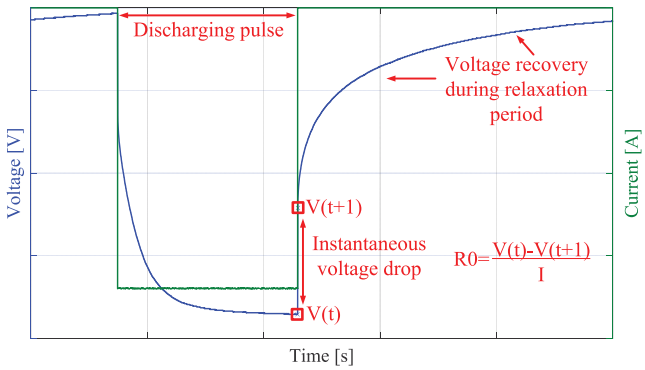

Fig. 7. The current pulse and its voltage response for the Li-S battery.

Finally, the ECM topologies with 1-4 R-C elements were compared by quantifying the sum-of-squared-errors (SSE) obtained during the fitting of relaxation voltage as well as by examining the SSE resulting from the simulation of the GITT profile.

$$SSE = \sum((V_{meas}(t) - V_s(t))^2) \tag{6}$$

where V_{meas} is the voltage profile measured in the laboratory and V_s is the voltage profile obtained from fitting or simulations.

C. The ECM validation

The most suitable ECM topology is selected and used for the model validation. The parameters dependency are integrated for 0.2, 0.5 and 1.0 C-rate. The validation was performed for 0.35 and 0.75 C-rate GITT profiles and the resulting voltage profiles are confronted with the measured ones.

V. Results & Discussion

A. ECM topology comparison

Four topologies with 1-4 R-C elements were parametrized by fitting the relaxation voltage. Afterward, the same current profile, which was applied for GITT procedure in the laboratory, was fed to the model, considering a one-second resolution.

The fitting accuracy of the relaxation voltage had an expected trend with more R-C elements the accuracy is increased. The example of voltage curves for 50% DOD is shown in Fig. 8. By comparing the SSE, which were obtained from fitting, and are summarized in Table III, one can observe that by moving from a 1 R-C ECM to a 2 R-C model, the SSE is reduced by an order of magnitude. By adding the third R-C element, the SSE is reduced nearly two times compared to 2 R-C. Expanding to 4 R-C elements, the model brings only a minor improvement to the fitting accuracy. However, these numbers are related only to fitting of the relaxation voltage after applied pulse.

The current GITT profile was applied to the parametrized models. The resulting voltage curves for the 0.2 C-rate case are presented in Fig. 9. The simulated voltage curves match accurately the voltage during relaxation periods for higher

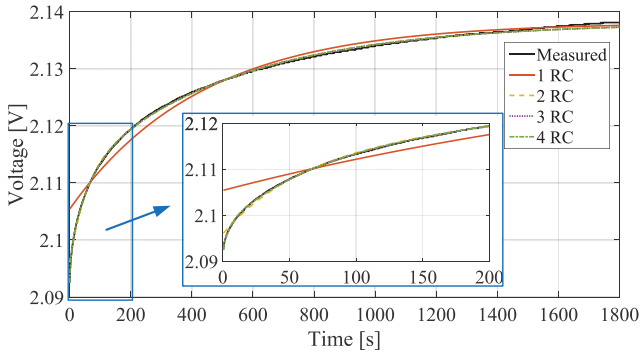

Fig. 8. The comparison of measured and fitted relaxation voltage for 0.2 C-rate at 50% DOD.

TABLE III. THE SSE COMPARISON FOR ECM TOPOLOGIES WITH 1-4 R-C ELEMENTS.

No. of R-C	SSE					
	fitting			GITT simulation		
	0.2 C	0.5 C	1.0 C	0.2 C	0.5 C	1.0 C
1 R-C	0.1736	0.2629	0.3342	7.9736	4.0169	2.9100
2 R-C	0.0181	0.0172	0.0231	1.9371	1.1589	1.5765
3 R-C	0.0095	0.0074	0.0094	0.6586	0.4544	1.2011
4 R-C	0.0093	0.0067	0.0078	3.0521	0.3842	1.2141

DOD states. In the low DOD stages, there is present a self-discharge process, as illustrated in Fig. 5, which was not implemented in the model and thus it caused a voltage estimation error. Nevertheless, the main error appearance is in the voltage response during the current pulse: 1 R-C ECM under-estimated and 4 R-C ECM over-estimated the voltage response. Moreover, the accuracy of 2 R-C element based ECM is reduced at high DOD stages.

The 3 R-C ECM, parametrized by the described method, had the best accuracy in estimating the measured voltage profile. This is reflected as well by SSEs of simulated and measured voltages in Table III, where the 3 R-C ECM has the lowest SSE. The 4 R-C ECM does not bring significant improvement to the model's accuracy and it increases the complexity of the model. The 2 R-C ECM has lower accuracy than the 3 R-C ECM, however if there is a need for low computational requirements, it might be a good trade-off solution. The 1 R-C based ECM simulation has, as expected, the highest SSE.

The 3 R-C ECM was selected for validation. All the derived parameters of the 3 R-C ECM are presented in Fig. 10-16.

B. ECM validation

Simulations with the GITT profiles of 0.35 and 0.75 C-rates, which were not used for parametrization, were performed in order to validate the developed Li-S battery model. The comparison between the measured and estimated voltage profiles is shown in Fig. 17 for the 0.35 C-rate and in Fig. 18 for the 0.75 C-rate. In both cases, the simulated voltage matches well the measured voltage at high DOD stages. However, for early discharge at low DOD there is visible a mismatch, which might be caused by not appropriately derived OCV values for the applied C-rates. This might be the result of not-accurate SOC computing due to the battery high dependance on C-rate,

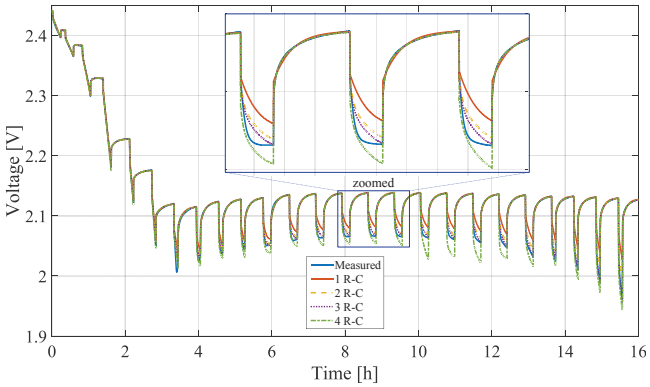

Fig. 9. The comparison of measured and simulated voltage for 0.2 C-rate GITT profile.

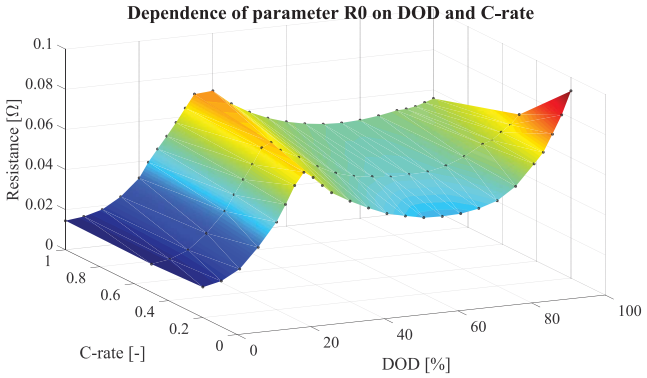

Fig. 10. Parameter R0 dependence on DOD and C-rate.

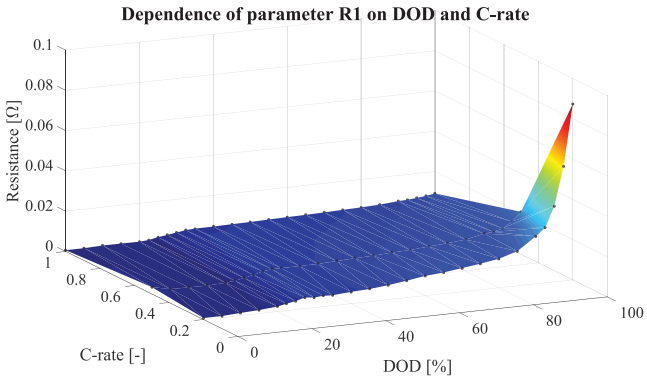

Fig. 11. Parameter R1 dependence on DOD and C-rate.

quick self-discharge in low DOD levels, coulombic efficiency farther from 100% or the result of ageing as the tests were done at different battery state-of-health stages. The obtained SSE values for the two validation tests are 3.9754 and 5.1440 for 0.35 and 0.75 C-rate, respectively.

The ECM of the Li-S battery with 3 R-C elements is considered validated for pulse-discharging operation with short relaxation periods by currents between 0.2 to 1.0 C-rate. The accuracy could be further improved by more consistent test for parametrization, which reduce the effect of ageing and it will include as well available capacity dependence on the applied C-rate. Moreover, including the self-discharge effect into the model would improve the model performance in high SOC stages.

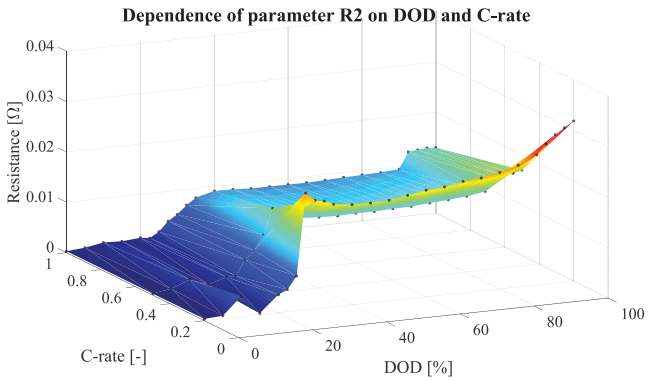

Fig. 12. Parameter R2 dependence on DOD and C-rate.

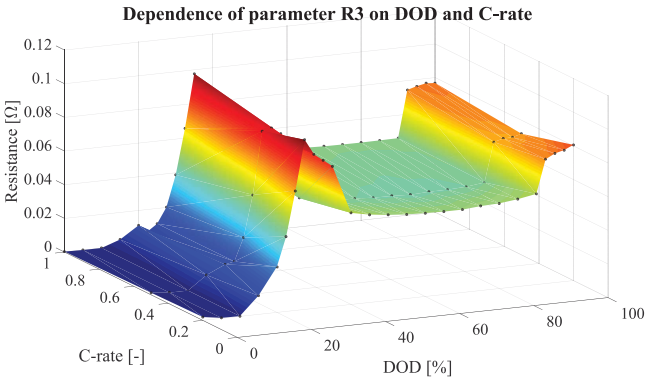

Fig. 13. Parameter R3 dependence on DOD and C-rate.

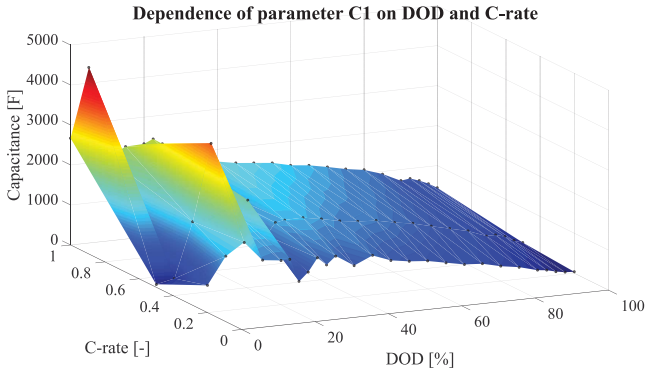

Fig. 14. Parameter C1 dependence on DOD and C-rate.

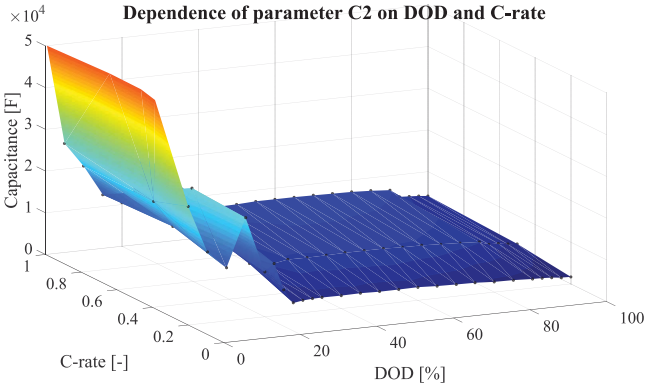

Fig. 15. Parameter C2 dependence on DOD and C-rate.

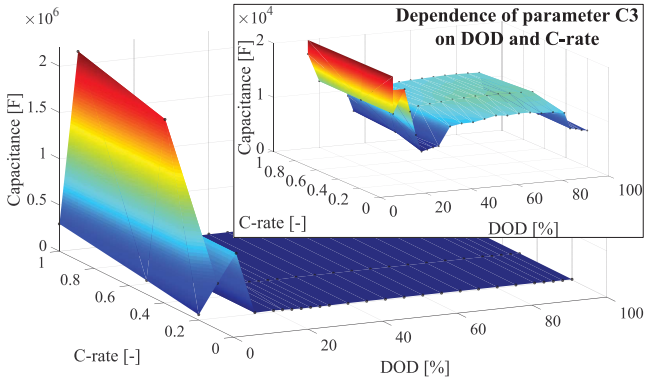

Fig. 16. Parameter C3 dependence on DOD and C-rate.

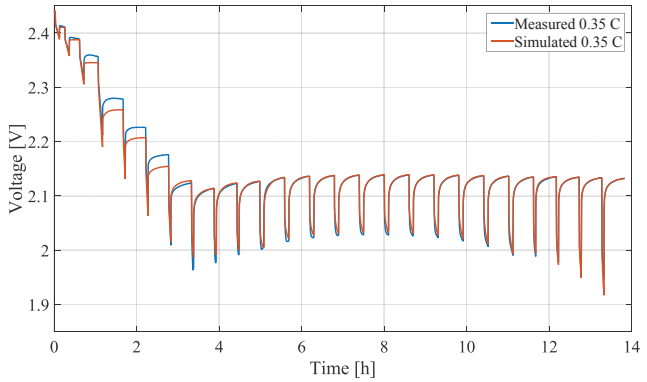

Fig. 17. The comparison of measured and simulated voltage for 0.35 C-rate.

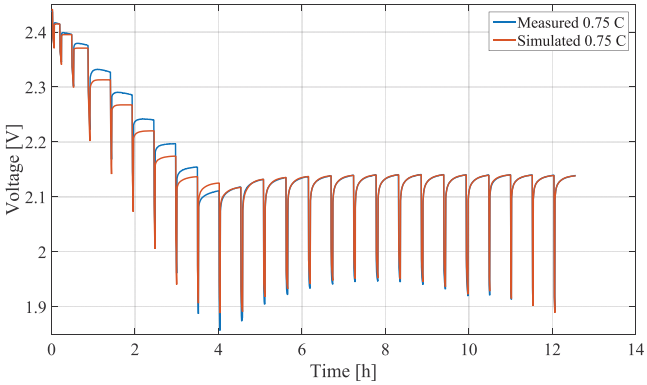

Fig. 18. The comparison of measured and simulated voltage for 0.75 C-rate.

VI. Conclusion

Different ECM topologies for the Li-S battery were summarized in this paper, together with their investigated dependencies on DOD and C-rate and the assigned physical meaning of the circuit elements. ECMs composed of one to four R-C elements were parametrized based on laboratory measurements performed on a 3.4 Ah Li-S pouch cell. The same GITT profile, which was used for the parametrization, was used as the input for the model simulation. The error of the fitting and the error from the simulations were evaluated and as the most suitable, the ECM with 3 R-C elements was selected for validation. For the validation process, the profiles from laboratory measurements with 0.35 and 0.75 C-rates were used. The main inaccuracies were caused by the inadequate determination of the OCV curve for the validation C-rates.

Only the discharging mode was implemented to the model. As a future work, the model should include the temperature dependence, be able to operate in charging mode and predict more accurately the response during discharging pulses.

ACKNOWLEDGMENT

This work has been part of the ACEMU-project (1313-00004B). Authors gratefully acknowledge the Danish Council for Strategic Research and EUDP for providing financial support and thank OXIS Energy for supplying the Lithium-Sulfur battery cell.

REFERENCES

[1] D. Bresser, S. Passerini, and B. Scrosati, "Recent progress and remaining challenges in sulfur-based lithium secondary batteries - a review," *Chem. Commun.*, vol. 49, no. 90, pp. 10 545–10 562, Nov. 2013.

[2] X. Hu, S. Li, and H. Peng, "A comparative study of equivalent circuit models for Li-ion batteries," *J. Power Sources*, vol. 198, no. 0, pp. 359 – 367, 2012.

[3] A. Seaman, T.-S. Dao, and J. McPhee, "A survey of mathematics-based equivalent-circuit and electrochemical battery models for hybrid and electric vehicle simulation," *J. Power Sources*, vol. 256, pp. 410–423, Jun. 2014.

[4] M. Einhorn, F. V. Conte *et al.*, "Comparison, selection, and parameterization of electrical battery models for automotive applications," *IEEE Trans. Power Electron.*, vol. 28, no. 3, pp. 1429–1437, 2013.

[5] V. Kolosnitsyn, E. Kuzmina, and E. Karaseva, "On the reasons for low sulphur utilization in the lithium-sulphur batteries," *J. Power Sources*, vol. 274, pp. 203–210, Jan. 2015.

[6] K. Somasundaram, O. Neill, M. Marinescu *et al.*, "Towards an operational model for a Li-S battery," Poster, London, Sep. 2014.

[7] Z. Deng, Z. Zhang *et al.*, "Electrochemical Impedance Spectroscopy Study of a Lithium/Sulfur Battery: Modeling and Analysis of Capacity Fading," *J. Electrochem. Soc.*, vol. 160, no. 4, pp. A553–A558, Jan. 2013.

[8] C. Barchasz, J.-C. Leprêtre *et al.*, "New insights into the limiting parameters of the Li/S rechargeable cell," *J. Power Sources*, vol. 199, pp. 322–330, Feb. 2012.

[9] L. Yuan, X. Qiu, L. Chen, and W. Zhu, "New insight into the discharge process of sulfur cathode by electrochemical impedance spectroscopy," *J. Power Sources*, vol. 189, no. 1, pp. 127–132, Apr. 2009.

[10] Q. Tang, Z. Shan, L. Wang, X. Qin, K. Zhu, J. Tian, and X. Liu, "Nafion coated sulfurcarbon electrode for high performance lithiumsulfur batteries," *J. Power Sources*, vol. 246, pp. 253–259, Jan. 2014.

[11] V. Kolosnitsyn, E. Kuzmina, and S. Mochalov, "Determination of lithium sulphur batteries internal resistance by the pulsed method during galvanostatic cycling," *J. Power Sources*, vol. 252, pp. 28–34, Apr. 2014.

[12] B. H. Jeon, J. H. Yeon, and I. J. Chung, "Preparation and electrical properties of lithium-sulfur-composite polymer batteries," *J. Mater. Process. Technol.*, vol. 143-144, pp. 93–97, Dec. 2003.

[13] V. Kolosnitsyn, E. Kuzmina *et al.*, "A study of the electrochemical processes in lithium-sulphur cells by impedance spectroscopy," *J. Power Sources*, vol. 196, no. 3, pp. 1478–1482, Feb. 2011.

[14] G. Ma, Z. Wen, Q. Wang, C. Shen, J. Jin, and X. Wu, "Enhanced cycle performance of a Li-S battery based on a protected lithium anode," *J. Mater. Chem. A*, vol. 2, no. 45, pp. 19 355–19 359, Sep. 2014.

[15] M. Barghamadi, A. Kapoor, and C. Wen, "A Review on Li-S Batteries as a High Efficiency Rechargeable Lithium Battery," *J. Electrochem. Soc.*, vol. 160, no. 8, pp. A1256–A1263, May 2013.

[16] Y. V. Mikhaylik and J. R. Akridge, "Polysulfide Shuttle Study in the Li/S Battery System," *J. Electrochem. Soc.*, vol. 151, no. 11, p. A1969, 2004.

[17] N. a. Cañas, K. Hirose, B. Pascucci *et al.*, "Investigations of lithium-sulfur batteries using electrochemical impedance spectroscopy," *Electrochim. Acta*, vol. 97, pp. 42–51, May 2013.

[18] J. Zhang, Z. Dong, X. Wang, X. Zhao, J. Tu, Q. Su, and G. Du, "Sulfur nanocrystals anchored graphene composite with highly improved electrochemical performance for lithium-sulfur batteries," *J. Power Sources*, vol. 270, pp. 1–8, Dec. 2014.

[19] Z. Shen, L. Cao, C. D. Rahn, and C.-Y. Wang, "Least Squares Galvanostatic Intermittent Titration Technique (LS-GITT) for Accurate Solid Phase Diffusivity Measurement," *J. Electrochem. Soc.*, vol. 160, no. 10, pp. A1842–A1846, 2013.

[20] L. W. Yao, J. a. Aziz, P. Y. Kong, and N. R. N. Idris, "Modeling of lithium-ion battery using MATLAB/simulink," *IECON Proceedings (Industrial Electronics Conference)*, pp. 1729–1734, 2013.

[21] V. Knap, D.-I. Stroe, R. Teodorescu, M. Swierczynski, and T. Stanciu, "Comparison of Parametrization Techniques for an Electrical Circuit Model of Lithium-Sulfur Batteries," in *Industrial Informatics (INDIN), 2015 13th IEEE International Conference on*, July 2015.